

## Characterization of a hybrid photon-counting detector based on Timepix4 with a quasi-monochromatic source for spectral X-ray imaging applications

V. MAZZINI<sup>(1)(2)(\*)</sup>, S. VELARDITA<sup>(1)</sup>, N. BIESUZ<sup>(1)</sup>, R. BOLZONELLA<sup>(1)(2)</sup>,  
V. CAVALLINI<sup>(1)(2)</sup>, L. CIMMINO<sup>(3)</sup>, M. FIORINI<sup>(1)(2)</sup>, R. LONGO<sup>(4)</sup>, V. ROSSO<sup>(5)</sup>,  
A. TAIBI<sup>(1)(2)</sup>, S. TUDISCO<sup>(6)</sup> and P. CARDARELLI<sup>(1)</sup>

<sup>(1)</sup> INFN Sezione di Ferrara - Ferrara, Italy

<sup>(2)</sup> Dipartimento di Fisica e Scienze della Terra, Università di Ferrara - Ferrara, Italy

<sup>(3)</sup> Dipartimento di Fisica, Università di Napoli and INFN Sezione di Napoli - Napoli, Italy

<sup>(4)</sup> Dipartimento di Fisica, Università di Trieste and INFN Sezione di Trieste - Trieste, Italy

<sup>(5)</sup> Dipartimento di Fisica, Università di Pisa and INFN Sezione di Pisa - Pisa, Italy

<sup>(6)</sup> INFN Laboratori Nazionali del Sud - Catania, Italy

received 31 January 2025

**Summary.** — Photon-counting technology offers the potential for substantial transformations in the field of X-ray medical imaging by the implementation of spectral techniques. Hybrid photon-counting detectors, based on a Timepix4 ASIC coupled with a silicon sensor, were studied. A preliminary characterization of the X-ray energy response was performed using a quasi-monochromatic X-ray irradiation setup. This system, developed at University of Ferrara, is based on Bragg's diffraction by a mosaic crystal and it is capable of providing X-rays with energy tunable between 8 and 35 keV. This contribution presents the characterization of the irradiation system and preliminary tests to study the detector response to radiation.

### 1. – Introduction

Photon-counting technology represents a major leap in X-ray imaging, contributing to improved contrast-to-noise ratios, superior spatial resolution, and refined spectral imaging [1]. The Timepix4 hybrid pixel photon-counting detector [2] features a  $448 \times 512$  pixel array, bump-bonded to a sensor that can be selected based on experimental requirements. In this work, a  $500 \mu\text{m}$  silicon sensor with a  $55 \mu\text{m}$  pixel pitch was used. This technology is very promising in spectral imaging applications, providing continuous energy spectrum images even in high-rate environments (up to  $\sim 4 \times 10^6$  hits/ $\text{mm}^2/\text{s}$ ) [2]. With this type of technology, an absolute energy calibration of the response is necessary, and this is typically done by employing an intense monochromatic X-ray source, using systems such as synchrotrons [3]. However, the creation of an equivalent system that

(\*) E-mail: mzzvtr@unife.it

is accessible in a laboratory setting and cost-effective is of significant interest. One solution that has already been employed successfully is the use of X-ray fluorescence photons from selected materials, as demonstrated in previous studies [3, 4]. We used an alternative X-ray system, which was previously developed for archaeometry and medical applications [5], to evaluate the energy response of our detector. The system, located in the Larix-A laboratory of the University of Ferrara and INFN section of Ferrara, is based on a mosaic crystal and Bragg's diffraction to obtain a quasi-monochromatic X-ray beam. It has been fully characterized and employed to irradiate the Timepix4 detector to study its radiation response.

## 2. – Materials and methods

The experimental setup, shown in fig. 1(a), is designed to use Bragg's diffraction for generating a quasi-monochromatic beam, employing a  $\theta - 2\theta$  configuration to maintain the angle between the crystal and the X-ray tube at  $\theta_B$  [5]. The setup features a XM 12 mammographic X-ray tube (I.A.E., Italy), with a rotating molybdenum anode and a nominal focal spot size of  $0.3 \text{ mm}^2$ . At the tube exit, the primary beam is collimated by three lead slits, each 2 mm wide. To select the energy, we used a highly oriented pyrolytic graphite mosaic crystal (Optigraph Ltd, Moscow, Russia), by changing the reflection angle. The refracted beam is collimated by two lead slits after the mosaic crystal to avoid scattering and absorb the primary (non-refracted) beam.

**2.1. Characteristics of the irradiation field.** – The system was carefully set and aligned to obtain mean energy values ranging from 8 to 35 keV. The spatial positioning of the beam was studied using the RadEye100 X-ray high-resolution imaging detector (Rad-Icon Imaging Corp, CA, USA), while the energy distributions were measured with an XR-100T CZT detector (Amptek, MA, USA), with a lead collimator having a circular aperture with  $\phi = 1 \text{ mm}$ . The normalized spectra are presented in fig. 1(b). Smaller peaks, corresponding to second harmonic peaks resulting from Bragg's law, are noticeable at lower energies. However, these do not pose any issue, as they are easily distinguishable from the first harmonic within this energy range both in the measurements with Amptek CZT and Timepix4 detector. To determine the energy values, we applied a Gaussian fit to the energy peaks, to extract both the mean value ( $E_{CZT}$ ) and the standard deviation ( $\sigma_{CZT}$ ), as detailed in table I. In fig. 1(b), the spread of the spectra is dominated by the mosaic spread ( $0.28^\circ$ ). It was verified that the spatial change of the mean energy of the

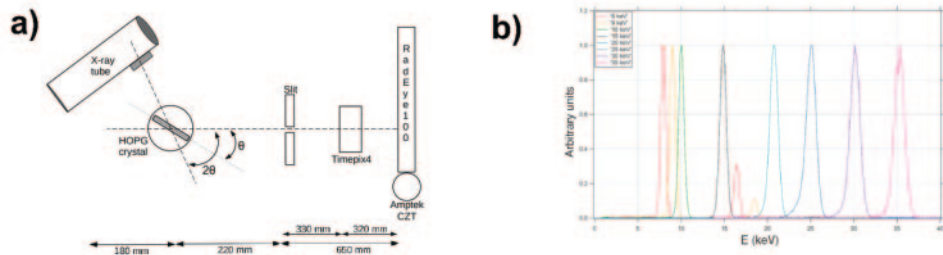


Fig. 1. – (a) Schematics of experimental setup. Radeye100, Amptek CZT and Timepix4 detectors are mounted on mobile platforms. (b) Normalized energy spectra of the quasi-monochromatic beam.

TABLE I. – Nominal energy values ( $E_{nom}$ ), used to calculate Bragg’s angle ( $\theta_B$ ), and Gaussian fit results ( $E_{CZT}$ ,  $\sigma_{CZT}$ ) for the Amptek CZT detector energy distribution.

$E_{nom}$ (keV)	$\theta_B$ (°)	$E_{CZT}$ (keV)	$\sigma_{CZT}$ (keV)
8	13.6	7.9	0.3
9	11.9	9.0	0.2
10	10.7	9.9	0.4
15	7.1	14.9	0.5
20	5.3	18.4	0.4
25	4.2	25.3	0.6
30	3.5	30.4	0.7
35	3.0	34.7	0.8

beam as a function of position over a few millimeters is negligible with respect to the local energy spread. The energy bandwidth ( $FWHM/E$ ), representing the relative energy spread, decreases from 9% to 4% with increasing beam energy. For these measurements a flux of the order of  $10^4$ – $10^5$  photons/mm<sup>2</sup>/s was used.

The spatial distribution of the beam intensity was studied. After collimation, the beam dimensions were  $0.9 \times 10$  cm. Figure 2(a) shows the beam as detected by the detection system.

**2.2. Timepix4 irradiation.** – For the preliminary Timepix4 energy calibration tests, we chose not to utilize the entire matrix to limit the volume of data and analysis time, instead focusing on three  $5 \times 5$  pixel clusters ( $275 \times 275 \mu\text{m}^2$ ) positioned near the center of the distribution, as shown in fig. 2(b). The sensor was calibrated pixel by pixel across its entire matrix using the Timepix4’s internal *test pulser*, allowing controlled injection of pulses with varying charges into individual pixels. This intrinsic calibration, as demonstrated in a previous study [4], was found to have limitations and to require an additional absolute calibration using an external X-ray source. Therefore, the detector was exposed to X-ray irradiation with the quasi-monochromatic system. We acquired the energy spectra for different mean energies, starting from 10 keV, up to 35 keV in 5 keV steps, resulting in histograms of the energy distribution for each energy value. With negligible positional effects across the 5 Timepix4 irradiation pixels and the CZT collimator aperture, all Timepix4 pixels observe the same spectrum as the Amptek CZT.

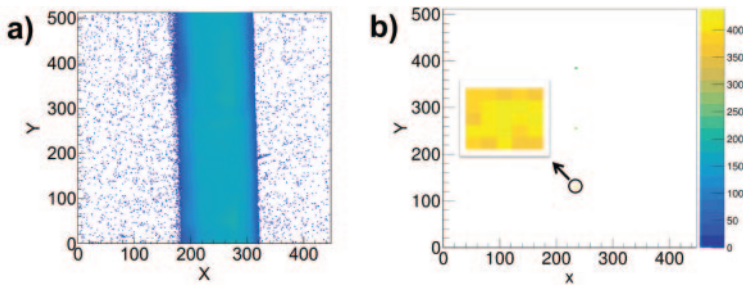


Fig. 2. – (a) Spatial distribution of the quasi-monochromatic beam. (b) Three pixel clusters of  $5 \times 5$  pixels used in the Timepix4 preliminary tests. The insert shows one of the clusters.

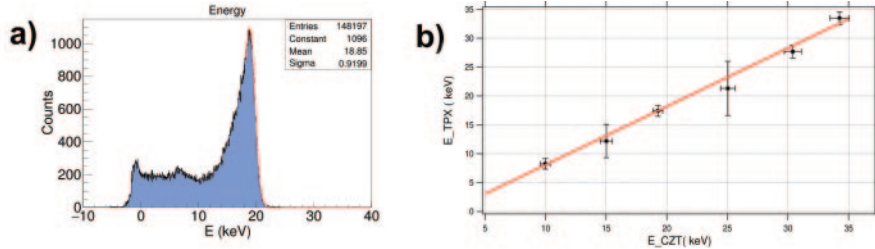


Fig. 3. – (a) Energy distribution at 20 keV. The red line represents the Gaussian fit. (b) Timepix4 energy  $E_{TPX}$  as a function of the Amptek CZT measurement ( $E_{CZT}$ ).

### 3. – Results

From the experimental campaign, six energy distributions were acquired, one of which is shown in fig. 3(a). An asymmetric Gaussian fit was applied to the observed peak, to determine the mean energy value and standard deviation ( $\sigma$ ), revealing an energy shift of a few keV relative to the Amptek CZT measurement ( $E_{CZT}$ ). Plotting the Timepix4 energy ( $E_{TPX}$ ) versus  $E_{CZT}$ , a linear calibration fit was obtained to correct the observed behavior, as shown in fig. 3(b). The  $x$ -axis uncertainty is represented by  $\sigma_{CZT}$ , while the  $y$ -axis uncertainty corresponds to the  $\sigma$  of the Gaussian fits applied to the Timepix4 energy spectra. The fit yielded a slope of  $a = 1.01$  and an intercept of  $b = -2.04$ . Although the slope being close to 1 indicates that no significant rescaling of the values is necessary, the negative intercept suggests a systematic energy offset. By applying a correction of 2.04 keV, the measured results  $E_{TPX}$  aligned more closely with the expected energy values ( $E_{CZT}$ ), reducing the discrepancy between the average energies below 4%.

### 4. – Conclusions

Preliminary tests of a 500  $\mu\text{m}$  silicon assembly coupled with the Timepix4 ASIC were performed using a functional and tunable X-ray quasi-monochromatic system developed and installed at the University of Ferrara. This experimental setup establishes a foundation for future experiments involving the characterization of new detector assemblies with different sensor materials (CdTe, GaAs) and the irradiation of the whole detector matrix for pixel-by-pixel calibration.

\* \* \*

This work was carried out in the context of the Medipix4 Collaboration based at CERN and was supported by the MEDIPIX4 project funded by the INFN-CSN5.

### REFERENCES

- [1] FLOHR T. *et al.*, *Phys. Med.*, **70** (2020) 126.
- [2] LLOPART X. *et al.*, *J. Instrum.*, **17** (2022) C01044.
- [3] DELOGU P. *et al.*, *Nucl. Instrum. Methods Phys. Res. Sect. A*, **1068** (2024) 169716.
- [4] FERUGLIO A. *et al.*, *Nuovo Cimento C*, **47** (2024) 314.
- [5] BALDELLI P. *et al.*, *Phys. Med. Biol.*, **50** (2005) 2225.